Random multiple scattering of ultrasound.   I.   Coherent and ballistic waves

Arnaud Derode,* Arnaud Tourin, and Mathias Fink

Laboratoire Ondes et Acoustique, Université Denis Diderot—Paris VII, ESPCI—CNRS (UMR 7587), 10 rue Vauquelin, 75005 Paris, France

This is the first article in a series of two dealing with the statistical moments of ultrasonic waves transmitted through a disordered medium with resonant multiple scattering. Only the first-order moment is considered here. An ultrasonic pulsed wave is transmitted from a point source to a 128-element receiving array through two-dimensional samples with various thicknesses. The samples consist of random collections of parallel steel rods immersed in water. Experimental results show that the ensemble-averaged transmitted wave forms ("coherent wave") exhibit a time-dependent frequency spectrum. Within the independent scattering approximation, this is well explained by individual resonances of the scatterers. The coherent wave only appears after ensemble averaging and has to be distinguished from the "ballistic wave," i.e., the first well-defined pulse that crosses the sample, which can be measured on every realization of disorder. A physical interpretation is given, which is based on the separation of the coherent wave between a rigid and a resonant contribution.

I. INTRODUCTION

Physical systems involving multiple scattering of various kinds of waves (electrons, ultrasound, electromagnetic, or seismic waves, etc.) can be analyzed with very much the same concepts [1–7]. Whatever the type of waves, the statistical approach consists of treating a given multiple scattering medium as one realization of a random process. One aims at evaluating the statistical moments of the scattered waves in order to identify relevant parameters to characterize the medium (mean free paths, diffusion constant, transport velocity, conductance, . . .) and to explain the various phenomena of multiple wave scattering in disordered systems (coherent backscattering, conductance fluctuations, localization).

The major difference between acoustics and optics or quantum physics does not lie in the physical concepts, but rather in the physical quantity at stake in an actual experiment: Is it the instantaneous fluctuations of the field, or a time-averaged intensity? Is the incoming wave a broadband pulse or a quasi-monochromatic plane wave packet? Is there a rapid motion of the scatterers, or is the disorder fixed? Can the system be considered as ergodic?

In this work we will study the transmission of an ultrasonic pulsed wave from a point source to a 128-element receiving array through a multiple scattering slab. This slab is a two-dimensional (2D) sample consisting of a random collection of parallel steel rods immersed in water. Unlike optical wave scattering by suspensions, there is no Brownian motion here: one set of 128 transmitted wave forms corresponds to one realization of disorder, hence there is no "self-averaging." A key question is then to understand what information can be retrieved from the observation of a single realization, and what is revealed by an ensemble average. The answer to this question will be different according to

whether we are dealing with first- or second-order moments of the scattered wave, and will depend on the essential parameters of multiple scattering (Thouless factor, mean free paths).

This work is divided into two articles. The present paper deals with the first-order moment of the transmitted wave. The influence of individual resonant scattering on the ensemble-averaged wave forms is shown experimentally and well explained within the independent scattering approximation (ISA) [2]. We emphasize the difference between the "ballistic wave" i.e., the first well-defined pulse that crosses the sample appearing on a single realization of disorder, and the "coherent wave" that requires ensemble averaging.

II. EXPERIMENTS

The experimental situation we consider is depicted on Fig. 1. A subwavelength piezoelectric element transmits a short ultrasonic pulse (one or two cycles of a 3.2 MHz sine wave) that propagates through water and encounters a mul-
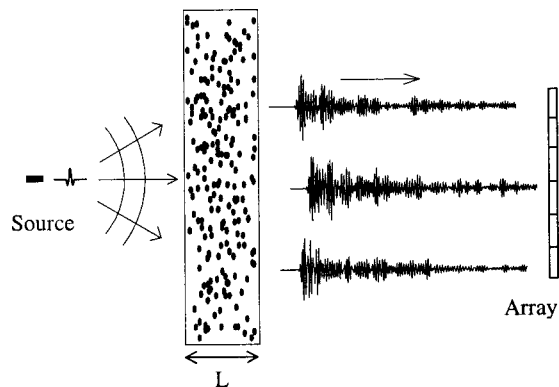

FIG. 1. The source transmits a short pulse that propagates through the slab. The scattered waves are recorded on a 128-element array. The sample can be translated parallel to the array for ensemble averaging.

─────────
*Author to whom correspondence should be addressed. Fax: 33 1 40 79 44 68; electronic address: arnaud.derode@espci.fr
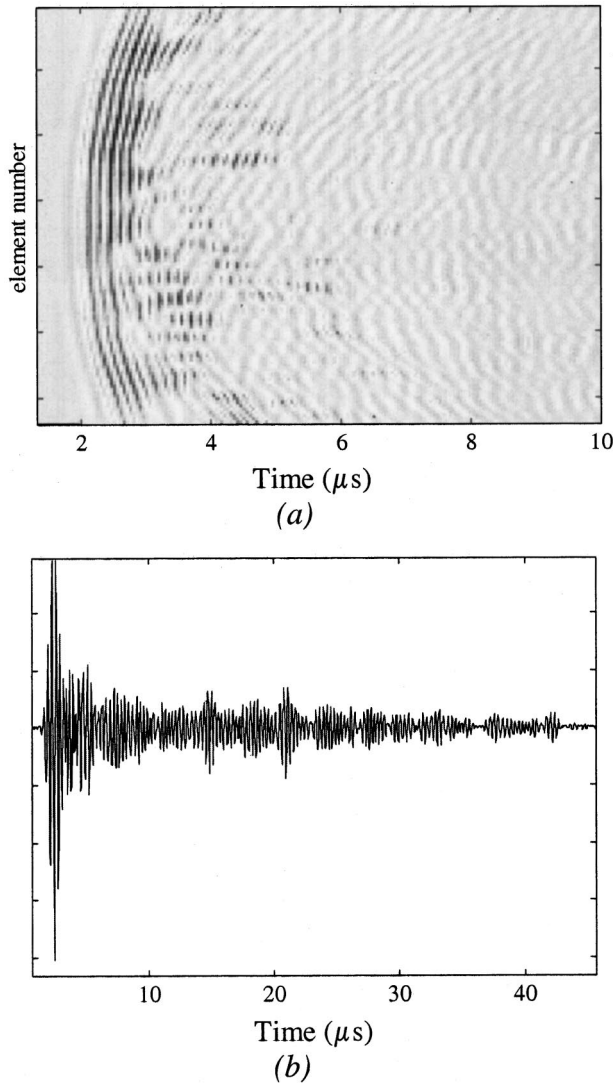
(a)

(b)

FIG. 2. (a) Transmitted wave forms for $L=10$ mm. The ballistic front dominates the scattered contributions. Each of the 128 lines of the picture corresponds to one array element. (b) Waveform received on element number 64. The time origin is arbitrary.

FIG. 3. Signal received on the array element No. 64, for $L=80$ mm. The time origin is arbitrary.

tiple scattering slab with thickness L. The slab is made of a random collection of parallel steel rods with density 18.75/cm^2 and diameter 0.8 mm (for comparison, the average wavelength in water is 0.47 mm). The receiving array has 128 0.39-mm large elements. The vertical dimensions of the rods and of the array are sufficiently larger than the wavelength to consider the setup as two dimensional. Scattered waves emerge from the sample and the array records 128 time series. Unlike in optics, the electrical signals that are recorded are a direct measurement of the field itself, not its intensity.

The scattered wave forms and the order of multiple scattering strongly depend on the sample thickness L. In our sample, the transport mean free path ℓ^* was found to be 4.8 mm, via the coherent backscattering effect [8]. For values of L comparable to ℓ^*, as in the case presented in Fig. 2, multiple scattering is not predominant: first, a cylindrical wave front traverses the sample. It has propagated at the
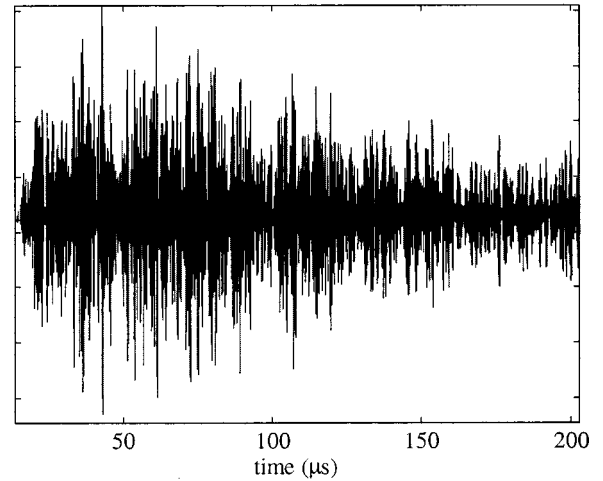
same velocity as in water, as if it had not felt the scatterers. This pulse is sometimes called ''ballistic wave'' [9,10]. After the ballistic front, there are low-level scattered contributions that fluctuate from one element to the other.

When the sample thickness increases, the amplitude of the ballistic front becomes smaller while the other contributions grow and last longer. For very large thickness (Fig. 3) the ballistic part is negligible, high-order multiple scattering dominates, and the transmitted signal lasts 200 or 300 μs, i.e., 300 times the initial pulse duration.

Given the complexity of the problem (at $L=80$ mm, roughly 1500 scatterers are involved) and the high order of scattering, it is impossible to give an analytical prediction of the wave transmitted through the slab. Usually, one considers a given sample as one particular realization of a random process and studies the first-order moment of the scattered wave (i.e., the ensemble-averaged transmitted field), also referred to as the coherent wave. It is a well-known result of scattering and effective media theory that its energy decays exponentially with the sample thickness [11].

In the case of wave propagation in suspensions, the ensemble average is replaced by a time average that is achieved naturally within the medium by the Brownian movement of the scatterers. On the contrary, in the situation we study here, the scatterers' positions are fixed, and we only have access to one realization at a time. Ideally, we would have to build another sample with different scatterers' positions obeying the same statistics, and repeat the experiment. In fact, to simulate an ensemble average the slab is translated parallel to the array until the transmitted signals are found to be decorrelated. This has been done for 70 positions, yielding 70 realizations of the transmitted wave.

When performing the ensemble average, a cylindrical wave front clearly emerges from the multiply scattered waves even when no ballistic front was clearly visible on a single realization of disorder: Figure 4(b) displays the experimental observation of the coherent wave for $L=30$ mm. And there is more to it than a simple ''ballistic wave:'' behind the first arrival, other wave fronts remain despite the ensemble averaging. Note that the frequency spec-
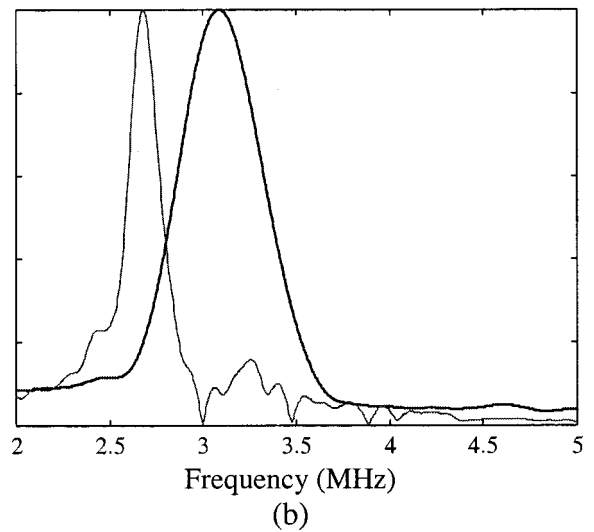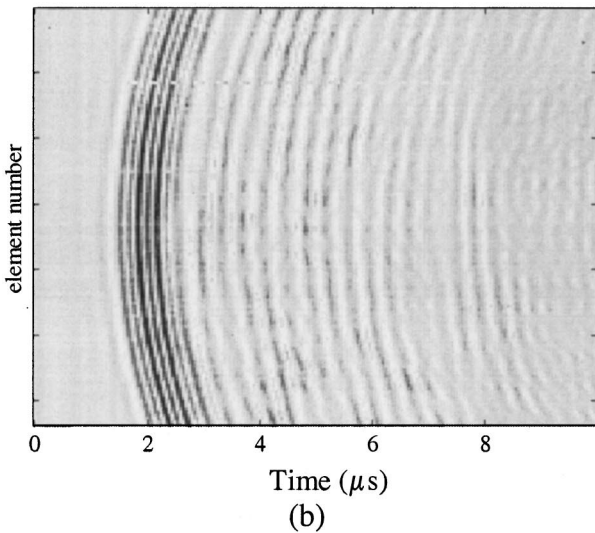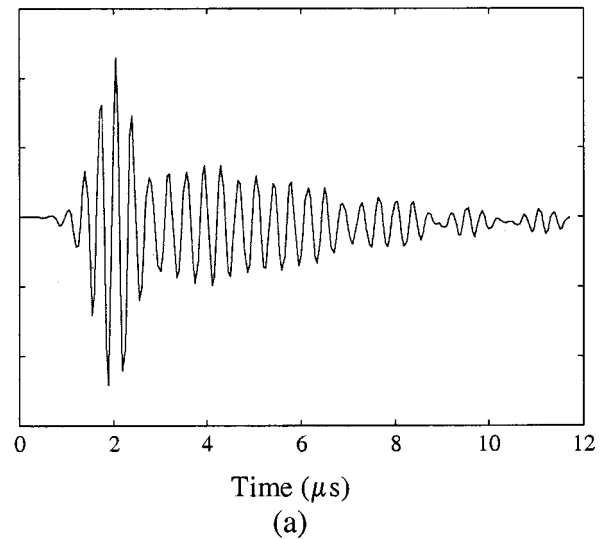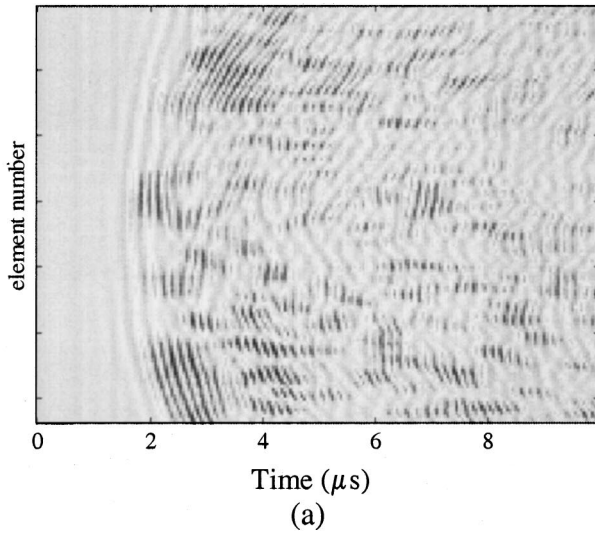
FIG. 4. (a) Transmitted wave forms though a slab with $L = 30$ mm, for one realization of disorder; the ballistic front is not predominent. (b) Ensemble-averaged transmitted wave forms for $L = 30$ mm: in addition to the ballistic contribution, secondary wave fronts are visible. Each of the 128 lines of the pictures corresponds to one array element.

FIG. 5. Experimental results. (a): Coherent wave form transmitted through $L = 30$ mm. (b): spectra of the early part (first 2.7 μs, thick line) and of the last part of the coherent signal (thin line).

trum of these secondary arrivals is significantly different from that of the earlier part (Fig. 5.).

III. THEORETICAL ANALYSIS AND DISCUSSION

In order to give a theoretical interpretation of this experimental result, the first step is to consider the scattering properties of one scatterer. For an elastic rod insonified by a plane wave, the total pressure may be written as the sum of the incoming wave and a scattered contribution which may be decomposed into a modal sum [12,13]:

$$e^{-j(\omega t - \mathbf{k_0} \cdot \mathbf{r})} + \sum_{n=0}^{\infty} a_n H_n^{(1)}(k_0 r) \cos(n\varphi) e^{-j\omega t}, \quad (1)$$

r is the distance from the center of the cylinder, φ the azimuth, k_0 the wave number in water, and the coefficients a_n are related to the boundary conditions at the cylinder surface; they depend on the longitudinal and transverse velocity, density, and radius of the cylinder.

In the far field, the scattered wave [second term in Eq. (1)] simplifies into a cylindrical wave:

$$f(\varphi) \frac{e^{-j(\omega t - k_0 r)}}{\sqrt{r}}. \quad (2)$$

Classical scattering theory introduces concepts such as the scattering cross section and the t matrix. The scattering cross section σ is defined as

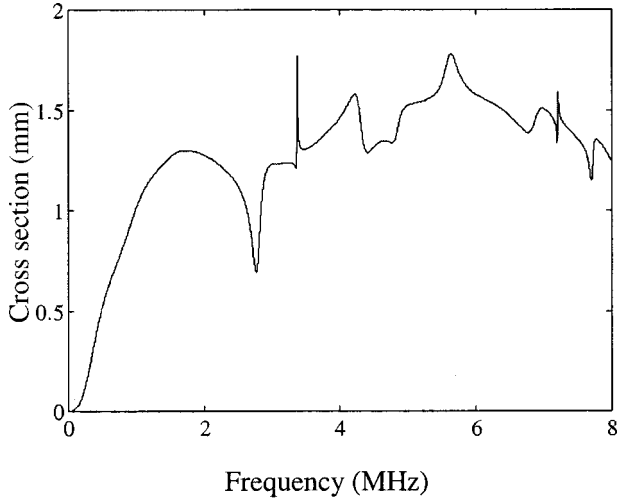$$\sigma = \int_0^{2\pi} |f(\varphi)|^2 d\varphi. \quad (3)$$

FIG. 6. Total scattering cross section (in mm) versus frequency (MHz), for a cylindrical steel rod with diameter 0.8 mm ($c_L = 5.7$ km/s, $c_T = 3$ km/s, $\rho = 7.8$).

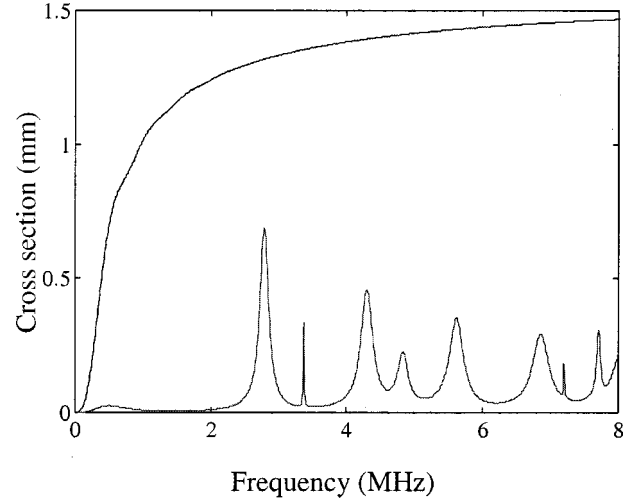

FIG. 7. Rigid and elastic scattering cross sections (in mm) versus frequency (MHz) for a cylindrical rod with diameter 0.8 mm ($c_L = 5.7$ km/s, $c_T = 3$ km/s, $\rho = 7.8$).

In a 2D problem such as this one, σ has the dimension of a length; it characterizes the scattering strength of the cylinder.

Alternatively, in the **k** space, scattering is described by a matrix t [14] that relates the outgoing plane wave component with wave vector **k** to the incoming plane wave, so that the matrix element $\langle \mathbf{k}|t|\mathbf{k}_0 \rangle$ is proportional to the scattered amplitude in the direction $\varphi = (\mathbf{k}_0, \mathbf{k})$. In the far field, the scattered amplitude $f(\varphi)$ and the t matrix are related by

$$f(\varphi) = -\frac{1+j}{4\sqrt{\pi k_0}} \langle \mathbf{k}|t|\mathbf{k}_0 \rangle. \tag{4}$$

Hence the t-matrix elements can be calculated from coefficients of the modal decomposition in Eq. (1):

$$\langle \mathbf{k}_0|t|\mathbf{k} \rangle = -4j \sum_{n=0}^{\infty} a_n \cos(n\varphi). \tag{5}$$

In particular, the scattered amplitude in the forward direction ($\varphi = 0$, $\mathbf{k} = \mathbf{k}_0$) is related to the total scattering cross section via the optical theorem [11]:

$$\sigma = -\frac{1}{k_0} \mathrm{Im}\langle \mathbf{k}_0|t|\mathbf{k}_0 \rangle = -\frac{4}{k_0} \mathrm{Re} \sum_{n=0}^{\infty} a_n. \tag{6}$$

Figure 6 displays the total scattering cross section σ versus frequency. The elastic parameters are $c_L = 5.7$ mm/μs, $c_T = 3$ mm/μs, $\rho = 7.8$, and the radius of the cylinder is 0.4 mm. After the low frequency (Rayleigh) regime, the curve shows rapid fluctuations. The peaks and dips in the total scattering cross section are both due to elastic resonances of the cylinder. Indeed the scattered amplitude may be split into a rigid and an elastic contribution:

$$f(\varphi) = f^{\mathrm{rig}}(\varphi) + f^{\mathrm{res}}(\varphi). \tag{7}$$

The rigid contribution f^{rig} is the response of a perfectly impenetrable object, while the elastic term f^{res} accounts for the

resonances linked to the geometry and the elasticity of the cylinder. It is therefore possible to write the total scattering cross section as a sum of three terms:

$$\sigma = \sigma^{\mathrm{rig}} + \sigma^{\mathrm{res}} + 2\,\mathrm{Re} \int f_{\mathrm{rig}}^*(\varphi) f_{\mathrm{res}}(\varphi) d\varphi. \tag{8}$$

The rigid and the elastic scattering cross sections are plotted in Fig. 7. While σ^{rig} grows monotonically with frequency and tends to a limit of 1.6 mm (twice the cylinder diameter), σ^{res} shows a series of peaks at particular frequencies (resonances).

The total scattering cross section is not the mere sum of σ^{rig} and σ^{res}, there is an interference term between the rigid and the resonant contributions. This is the reason why the strong resonance at 2.75 MHz manifests itself as a dip in the total scattering cross section. The resonances are the signatures of elastic surface waves propagating around the cylinder and reradiating a scattered wave into water: resonance occurs when a surface wave has an exact number of wavelengths around the cylinder. When waves reradiated by the surface wave are out of phase with the rigid term, resonance appears as a dip instead of a peak in the total scattering cross section, as was the case at 2.75 MHz.

The phase difference between the rigid and the elastic contributions may be thought of as the time necessary for the surface wave to be generated and reradiate a bulk wave in water, whereas the rigid response is almost instantaneous. As to the width of a given resonance, it can be related to the decay time of a surface wave that goes around the cylinder: as the surface wave reradiates, it is progressively attenuated. Therefore the width of the resonance can be linked to a "dwell time" of the surface wave around the cylinder [2].

From Fig. 7 its appears that in the frequency band we are interested in (~ 2–4 MHz), there are two resonance frequencies: 2.75 and 3.4 MHz. It should be noted that sharp resonances are very sensitive to the value of the rod radius a. Actually, the scattering cross sections depend on the dimen-
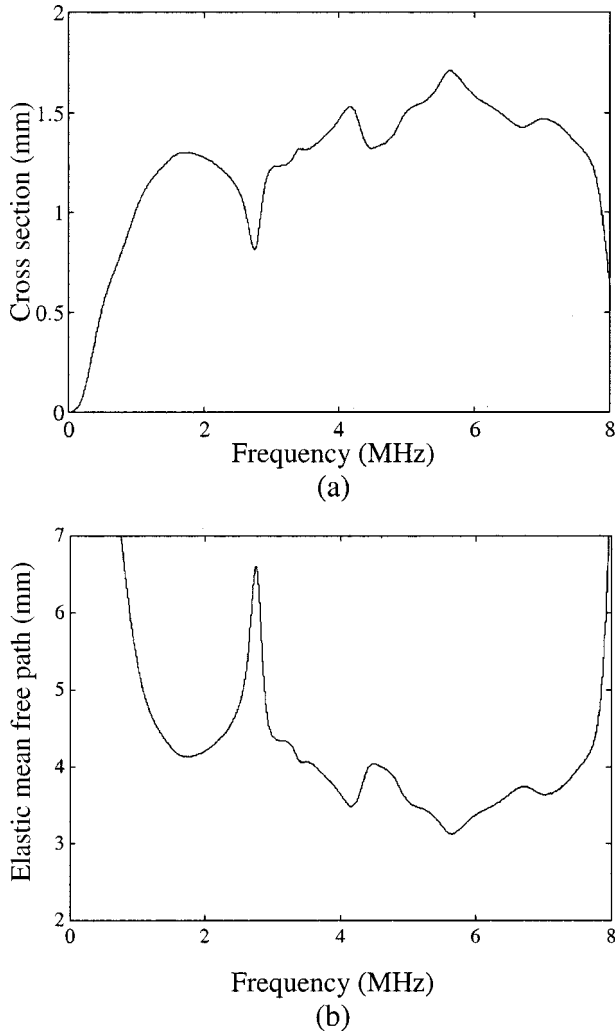
(a)

(b)

FIG. 8. Average scattering cross section (a) and elastic mean free path (b) in mm versus frequency (MHz) for a Gaussian distribution of radii (mean radius 0.4 mm, standard deviation 8 μm)

sionless parameter $k_0 a$. Therefore a small variation of the radius induces a change in the resonance frequencies. When considering an ensemble of rods, the scattered amplitude $f(\varphi)$ should be averaged in order to take the statistical distribution of the radii into account. This tends to smooth out the sharpest resonance. Figure 8 presents the average scattering cross section for a Gaussian distribution of rods with mean 0.4 mm and standard deviation 1/50 of the mean. Even this tiny fluctuation is enough to average out the sharp resonances.

In the frequency band between 2 and 4 MHz, only one resonance remains around 2.75 MHz. This resonance is the origin of the peculiar behavior of the coherent wave that was highlighted by the experiments.

Indeed, within the ISA [2], the ensemble averaged transmitted wave field when the slab is illuminated by a plane wave is written as

$$\langle H \rangle = e^{-j(\omega t - \mathbf{k}_{\text{eff}} \cdot \mathbf{r})}, \qquad (9)$$
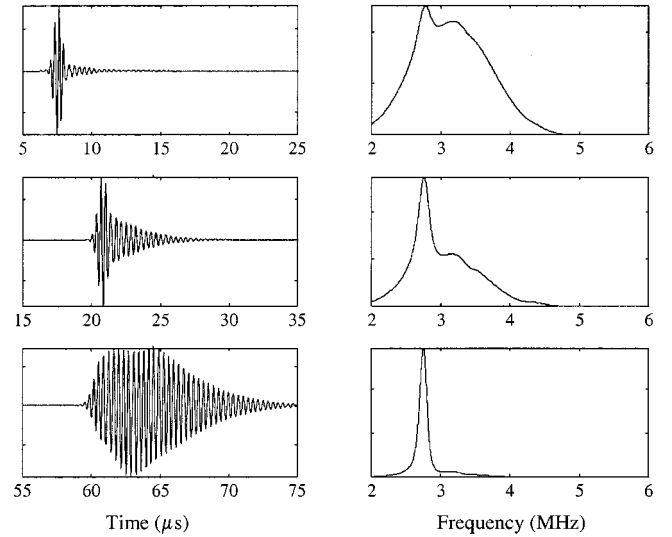
k_{eff} being the effective wave number:

FIG. 9. Theoretical results. Left column: coherent wave forms calculated within the ISA through $L=10$ mm (top), $L=30$ mm (middle), and $L=90$ mm (bottom). Right column: corresponding spectra.

$$k_{\text{eff}}^2 = k_0^2 - n \langle k_0 | t | k_0 \rangle. \qquad (10)$$

n is the density of scatterers (here, 18.75 cm^{-2}).

In the case of a plane wave insonification, the coherent wave is therefore a plane wave similar to the incoming one, with renormalized velocity and amplitude. In other words, on average the medium behaves as a filter with a frequency response $e^{jk_{\text{eff}}L}$. The real part of k_{eff} is related to the phase velocity of the effective medium, while its imaginary part is used to define the elastic mean free path:

$$\ell = \frac{1}{2 \, \text{Im}\{k_{\text{eff}}\}} \approx \frac{1}{n\sigma}. \qquad (11)$$

Since σ is minimal around 2.75 MHz, the mean free path and the frequency response show a maximum at this frequency (Fig. 8): $\ell = 4.1$ mm at 2 MHz, $\ell = 6.6$ mm at 2.75 MHz, and $\ell = 3.6$ mm at 4 MHz. And naturally, as the distance of propagation L increases, the frequency spectrum of the coherent wave narrows around the resonance frequency, 2.75 MHz.

In the time-domain we can calculate the coherent wave form via an inverse Fourier transform. As an example, the coherent wave form and its spectrum are plotted in Fig. 9 for various values of L. The incoming pulse spectrum has a 3.2 MHz center frequency and a 1.4 MHz full width at half maximum. For small values of L, the coherent wave form is essentially a ballistic contribution almost identical to the incoming pulse that seems to have propagated at the same velocity as in water.

But at larger L, the temporal wave form becomes more complicated: behind the first arrival, a second wave packet appears, with a different spectrum. For $L=30$ mm, a short-time Fourier analysis (Fig. 10) shows that the earlier part of the signal is centered at 3.1 MHz while the central frequency of the later part is the resonance frequency 2.75 MHz: the
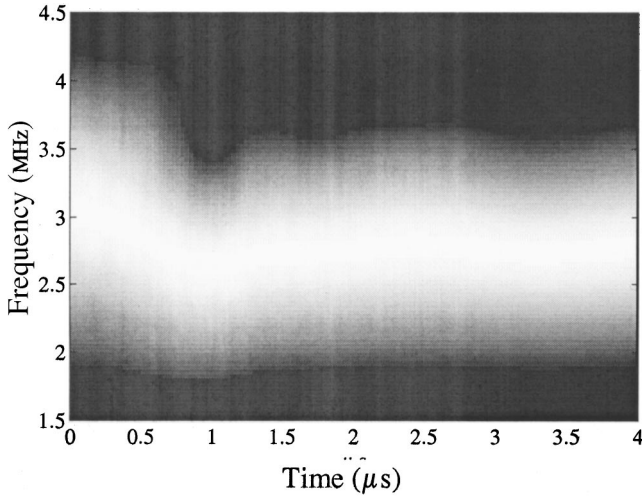
FIG. 10. Short-time Fourier analysis of the coherent waveform for $L = 30$ mm. Time (μs) is in the abscissa and frequency (MHz) on the ordinate. The mean frequency of the signal drops from 3.15 (ballistic part) to 2.75 MHz (resonant part).
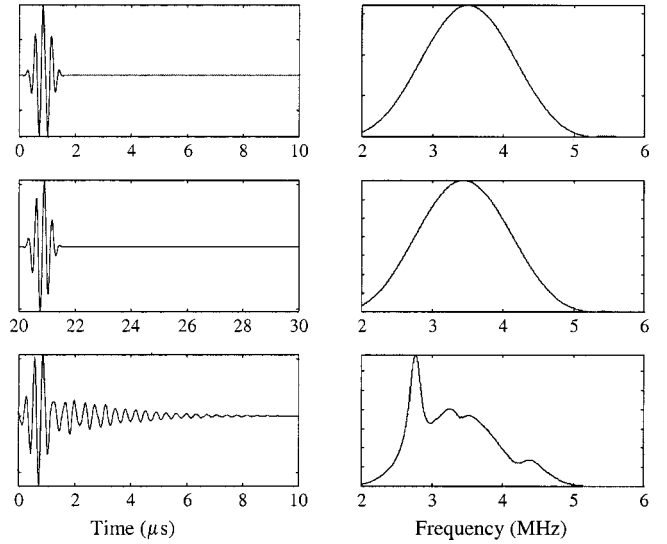

FIG. 11. Theoretical results. Left column: incoming signal (top), rigid response h_{rig} (middle), and resonant response (bottom) h_{res} for $L = 30$ mm. Right column: corresponding spectra.

travel time through the ensemble-averaged medium is strongly frequency dependent. In order to interpret this result, it may be useful to split once again the response of the medium between a rigid and an elastic contribution.

Under the approximation that $|n\langle k_0|t|k_0\rangle| \ll k_0^2$, we have

$$k_{\text{eff}} \approx k_0 - \frac{n\langle k_0|t|k_0\rangle}{2k_0}. \qquad (12)$$

Therefore the coherent wave can split into two terms:

$$\langle H \rangle = e^{-j(\omega t - \mathbf{k}_{\text{eff}} \cdot \mathbf{r})} = H_{\text{rig}} \times H_{\text{res}} \qquad (13)$$

or, alternatively, in the time-domain:

$$\langle h \rangle = FT^{-1} \langle H \rangle = h_{\text{rig}} \otimes h_{\text{res}} \qquad (14)$$

As we have seen in Fig. 7, the rigid cross-scattering section shows significant variations only in the low frequency (Rayleigh) regime. In the frequency bandwidth we consider (2–4 MHz), it is almost flat. Therefore the rigid frequency response is a constant, which means that the rigid part of the coherent wave is simply a replica of the incoming pulse, time shifted by $k_0 L/\omega$ (Fig. 11). This is the case each time resonances can be ignored, either because they are not present in the frequency bandwidth, or because they are averaged out by the statistical distribution of the scatterers radii. On the contrary, when the resonant behavior cannot be ignored, the coherent wave front spectrum appears as a filtered version of the incoming wave form, and spreads in time, which can be interpreted as a "dwell time" of the wave around the scatterer [2]. The dwell time of the wave can be estimated by computing the group delay associated to the coherent wave form. A comparison of the experimental and theoretical group delays are presented in Fig. 12. The group delays were calculated by convolving a quasi-monochromatic wave packet by the coherent wave form, and measuring the time difference between the maxima of the incoming and outgo-

ing wave packets. Naturally, the strong resonance around 2.7 MHz appears as a maximum in the group delay.

In the experimental results we presented the coherent signals were averaged over 70 realizations and 128 receivers. Is it possible to have at least a rough estimate of the mean free path from a single realization of disorder? It is, under two conditions: the ballistic signal has to be the essential contribution to the coherent wave, and the statistical fluctuations must be weak. Precisely, the amplitude of the coherent wave is $|\langle H \rangle| = e^{-L/2\ell}$. For sufficiently large samples, the mean value of the amplitude squared $\langle |H|^2 \rangle$ is well described by the diffusion approximation [4] and decays algebraically as ℓ^*/L. This result can be used to evaluate the variance of the transmitted wave H; the relative amplitude of the statistical fluctuations may then be estimated by $\sqrt{\text{var}(H)}/|\langle H \rangle| \approx \sqrt{\ell^*/L}e^{L/2\ell}$. In order to reduce the fluctuations to a ratio ε, the number of independent realizations to average is
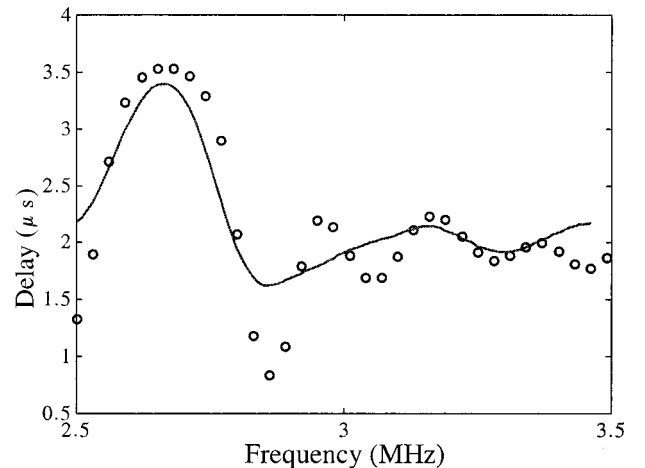

FIG. 12. Group delay (in μs) versus frequency, $L = 30$ mm. Continuous line: theoretical results derived from the ISA. Circles: experimental results. The time origin is arbitrary.

roughly $e^{L/\ell}\ell^*/L\varepsilon^2$. On the array we have at best 128 independent realizations: as soon as the sample thickness is more than one or two mean free paths, this it not enough to ensure a correct average. Yet another source of averaging lies in the fact that we have a large frequency bandwidth (this raises the question of frequency correlation, and the number of independent frequencies available in the transmitted signal, which will be dealt with in the next article). Taking advantage of the whole frequency bandwidth, experiments show that it is possible to measure a mean free path on a single realization of disorder, averaged over the frequency bandwidth, by considering the decay of the maximum of the ballistic pulse versus L, up to $L\sim4\ell^*$.

However, at larger thickness, averaging different realizations of disorder becomes necessary because the coherent wave can no longer emerge from a single realization. There are two reasons for this. One is that the propagation of the coherent wave becomes dispersive due to the resonance, so the initially well-defined pulse spreads more and more in time. The other reason is that as L increases the total amount of energy conveyed by the coherent wave becomes more and more negligible compared to that of the "incoherent" (diffuse) part of the transmitted signals.

IV. CONCLUSION

These results show that the coherent (or ensemble averaged) transmitted wave front bears information on the average scatterer inside the medium. Besides, it should be emphasized that the ballistic and the coherent wave forms are not the same thing: the ballistic part (the signal that seems to travel at the same velocity as in water and arrives first on each realization of disorder) contributes to the coherent part, but it is not the only contribution therein. The secondary wave forms that were observed experimentally on the coherent wave form are well explained within the ISA and are due to the presence of elastic resonance in the frequency bandwidth of interest. The response of the ensemble-averaged medium can be split into an "instantaneous" response that has the same spectrum as the incoming pulse, and a "delayed" response whose spectrum depend on the resonances that are not averaged out.

When the sample thickness L is not too large compared to the transport mean free path (up to $3\ell^*$), the ballistic wave is the essential contribution to the coherent wave, and resonant effects can be ignored. In that case it is possible to measure an elastic mean free path on a single realization of disorder, averaged over the frequency bandwidth, by considering the decay of the maximum of the ballistic pulse versus L. Yet, as soon as L is significantly larger than ℓ^*, the coherent wave is no longer reducible to the ballistic wave. The statistical fluctuations of the field around its mean value are so large that it becomes impossible to distinguish the coherent wave form on a single realization of disorder, even though it is "hidden" in the signals such as the one plotted in Fig. 3.

Moreover, it should be noted that the basic assumption of the ISA is that there are no correlations between the scatterers, which amounts to considering the slab as a dilute medium with no interaction between rods, like a perfect gas. In a dense scattering medium, this cannot be the case, since the scatterers have a finite size and cannot overlap, which will tend to give a certain degree of correlation between the scatterers' positions, like in Van Der Waals gas. The ISA is considered to be a reasonable approximation [2] as long as the scatterers' density does not exceed 10%; beyond that level, correlations between scatterers can no longer be neglected. In our case, the sample is just below this threshold (9.4% surfacic density), and the validity of the ISA is questionable. From the experiments, even though the scatterers are not pointlike and the medium is quite dense, the ISA seems to give correct results, at least for the first-order moment of the scattered field. Yet correlations between the scatterers should not be neglected, as we will emphasize in the next article.

[1] P. Sheng, *Introduction to Wave Scattering, Localization and Mesoscopic Phenomena* (Academic New York, 1995).

[2] A. Lagendijk and B. A. Van Tiggelen, Phys. Rep. **270**, 143 (1996).

[3] M. C. W. van Rossum and T. M. Nieuwenhuizen, Rev. Mod. Phys. **71**, 313 (1999).

[4] A. Z. Genack, in *Scattering and Localization of Waves in Random Media*, edited by Ping Sheng (World Scientific, Singapore, 1990), pp. 207–311.

[5] P. A. Lee and T. V. Ramakrishnan, Rev. Mod. Phys. **57**, 287 (1985).

[6] L. Margerin, M. Campillo, and B. van Tiggelen, Geophys. J. Int. **134**, 596 (1998).

[7] A. Tourin, M. Fink, and A. Derode, Waves Random Media **10**, R31 (2000).

[8] A. Tourin, A. Derode, A. Peyre, and M. Fink, J. Acoust. Soc. Am. **108**, 503 (2000).

[9] X. Jia, C. Caroli, and B. Velicky, Phys. Rev. Lett. **82**, 1863 (1999).

[10] R. Snieder and J. A. Scales, Phys. Rev. E **58**, 5668 (1998).

[11] A. Ishimaru, *Wave Propagation and Scattering in Random Media* (Academic, New York, 1978), Vols. 1 and 2.

[12] R. D. Doolittle, H. Uberall, and P. Ugincius, J. Acoust. Soc. Am. **43**, 1 (1968).

[13] N. Gespa, *Acoustic Scattering by Elastic Scatters with Simple Geometrical Shape* (Cedocar, Paris, 1987) (in French).

[14] D. Sornette, Acustica **67**, 199 (1989).